Charge dynamics in underdoped $Nd_{2-x}Ce_xCuO_4$: Pseudogap and related phenomena

Y. Onose
Spin Superstructure Project, Exploratory Research for Advanced Technology (ERATO), Japan Science and Technology Corporation (JST), Tsukuba 305-8562, Japan
and Department of Applied Physics, University of Tokyo, Tokyo 113-8656, Japan

Y. Taguchi* and K. Ishizaka
Department of Applied Physics, University of Tokyo, Tokyo 113-8656, Japan

Y. Tokura
Spin Superstructure Project, Exploratory Research for Advanced Technology (ERATO), Japan Science and Technology Corporation (JST), Tsukuba 305-8562, Japan,
and Department of Applied Physics, University of Tokyo, Tokyo 113-8656, Japan,
and Correlated Electron Research Center (CERC), National Institute of Advanced Industrial Science and Technology (AIST), Tsukuba 305-8562, Japan

(Received 2 May 2003; revised manuscript received 8 September 2003; published 9 January 2004)

We have investigated the temperature and doping variations of optical and transport properties in the electron-doped high-T_c cuprate crystals $Nd_{2-x}Ce_xCuO_4$ ($0 \leqslant x \leqslant 0.15$). In the optical spectra of underdoped crystals ($x < 0.15$), a notable pseudogap is observed at low temperatures. A Drude-like response evolves concomitantly with pseudogap formation. Both the magnitude (Δ_{PG}) and onset temperature (T^*) of the pseudogap decrease with electron doping, while holding the relation that $\Delta_{PG} \approx 10 k_B T^*$. The Δ_{PG} is comparable to the magnitude of the pseudogap at around $(\pi/2, \pi/2)$ in the photoemission spectra reported by Armitage *et al.* [Phys. Rev. Lett. **88,** 257001 (2002)], which indicates that the pseudogap appearing in the optical spectra is identical to that discerned by the photoemission spectroscopy. The scattering rate spectra $1/\tau(\omega)$ of the $x = 0.10-0.15$ crystals show a kink structure at around 0.07 eV, which can be ascribed not to the pseudogap but to the electron-phonon coupling. In accordance with the evolution of the Drude response, the in-plane resistivity begins to decrease rapidly at around T^* in the underdoped region. The out-of-plane resistivity shows an even more distinct decrease below T^*. This is because the interplane charge transport is governed by electronic states at around $(\pi, 0)$, where the quasiparticle spectral weight is accumulated in the case of the electron-doped system. This is contrary to the hole-doped case with the pseudogap around this point. The origin of the pseudogap has been ascribed to the antiferromagnetic spin correlation, which is consistent with the evolution of a two-magnon band in the B_{1g} Raman spectra below T^*. The pseudogap phenomenon in the electron-doped cuprate has been argued comparatively with that of the hole-doped cuprate.

DOI: 10.1103/PhysRevB.69.024504 PACS number(s): 74.72.Jt, 78.30.−j, 75.50.Ee, 74.25.Jb

I. INTRODUCTION

The unusual spin and charge dynamics in high-T_c cuprates have been attracting great interest. Especially, in the underdoped region of hole-doped cuprates, many anomalous features have been unveiled. At present, most of them are believed to be due to pseudogap formation.[1] There seems to be two types of pseudogaps: namely, a large-energy pseudogap and a small-energy one. The former has the energy scale of an antiferromagnetic interaction (J) and is observed around the $(\pi, 0)$ point of the Fermi surface by angle-resolved photoemission spectroscopy,[2–5] while the energy scale of the latter is comparable to that of the superconducting gap.[6–8] The characteristic temperature (T) dependences of the Hall coefficient[9,10] and magnetic susceptibility[11,12] are believed to be ruled by large-energy pseudogap formation. Smaller-energy pseudogap formation manifests itself also in the spin excitation spectra.[13,14] In spite of the vast numbers of experimental works on hole-doped cuprates, the origin of pseudogaps remains controversial.

The discovery of superconductivity in the electron-doped cuprate $Nd_{2-x}Ce_xCuO_4$ demonstrated presence of electron-hole symmetry in high-T_c superconductors.[15] This has laid a strong constraint on theories of the high-T_c mechanism.[16,17] Further comparative studies on the underdoped region of electron- and hole-doped systems may also provide useful information to examine controversial issues such as the pseudogap one. The ground state in the underdoped region of $Nd_{2-x}Ce_xCuO_4$ is different from that in the hole-doped system. While the superconductivity is induced by only 5% hole doping into the CuO_2 plane,[18] antiferromagnetic long-range order is robust up to $x \approx 0.14$ in $Nd_{2-x}Ce_xCuO_4$.[19] Nevertheless, some features are commonly observed in the underdoped region of both electron- and hole-doped systems (for example, T and doping variations of the Hall coefficient[9]).

We have investigated the charge transport characteristics and the optical spectra for the underdoped region of $Nd_{2-x}Ce_xCuO_4$. A large-energy pseudogap structure is observed in the optical conductivity spectra and the anomalies related to the pseudogap are manifested in the low-energy charge dynamics (Drude-like response in optical spectra and charge transport properties), some of which are common to

that in hole-doped systems.[20] A part of the results have been published in a form of short Letters.[22,23] In the present paper, we present the full results and a detailed analysis of the optical and transport data, including new findings of anomalies in the out-of-plane resistivity and the two-magnon Raman scattering spectra, all related to pseudogap formation. We show the close relation between the present results of the optical and transport measurements and the recent results of angle-resolved photoemission spectroscopy (ARPES).[24–26] As a compelling interpretation, the origin of pseudogap formation is ascribed to the *T*-dependent evolution of antiferromagnetic correlation. This is also evidenced by the *T* variation of the two-magnon peak in the Raman spectra. We also argue the similarities and differences of the normal-state charge dynamics and the pseudogap features between the electron-doped and hole-doped cuprates.

II. EXPERIMENT

Single crystals of $Nd_{2-x}Ce_xCuO_4$ ($x=0$, 0.025, 0.05, 0.075, 0.10, 0.125, and 0.15) were grown by the traveling-solvent floating-zone method at a rate of 0.6–1 mm/h in 4 atm O_2 atmosphere. The grown crystals were confirmed to be single crystals without any trace of secondary phase by measurements of powder patterns and Laue reflection of x rays. It was also confirmed by inductively coupled plasma atomic emission spectroscopy that the Ce concentration *x* is close to the prescribed value with an accuracy of ± 0.01. To avoid the influence of apical oxygen as the interstitial impurities,[27] all crystals except $x=0$ were annealed in a flowing Ar/O_2 gas mixture at 1000 °C for 100 h. The partial oxygen pressure of the Ar/O_2 gas was optimized so as to obtain the highest T_c or the lowest resistivity in the respective sample.

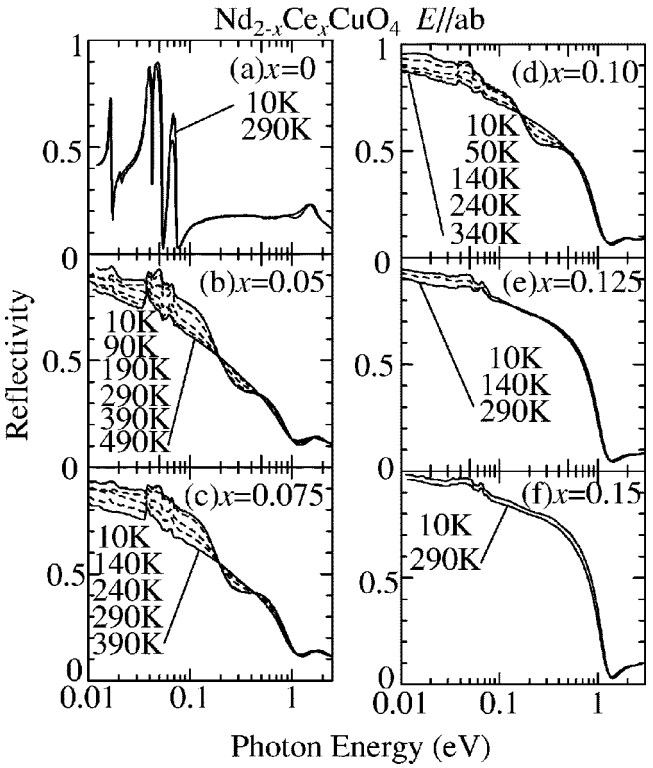

FIG. 1. In-plane reflectivity spectra at various temperatures for single crystals of $Nd_{2-x}Ce_xCuO_4$.

For the resistivity measurements, we cut the crystal boule into a rectangular shape with a typical size of $1\times2\times0.2$ mm^3, and a conventional four-probe method was em-

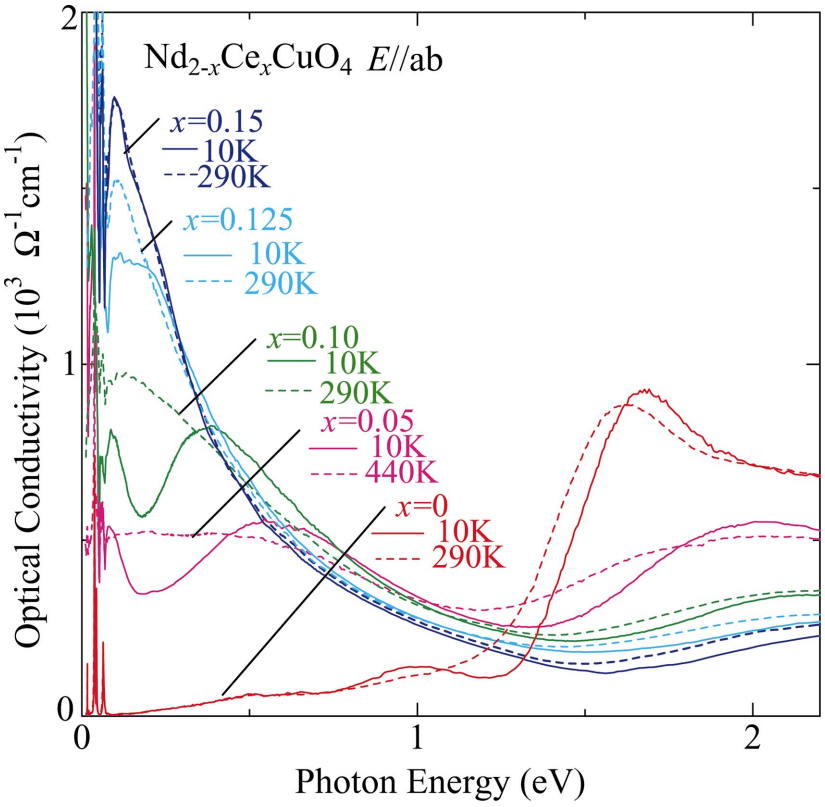

FIG. 2. (Color) Doping dependence of optical conductivity spectra for $Nd_{2-x}Ce_xCuO_4$ crystals with $x=0$–0.15 at 10 K and a sufficient high temperature (440 K for the $x=0.05$ crystal and 290 K for the others).

ployed. To deduce the optical conductivity spectra, reflectivity spectra were measured on the *ab* face of crystals with typical size of $4\times4\times1$ mm^3. For this measurement, the surface was polished with alumina powder to a mirrorlike surface. To remove possible residual stress at the polished surface, we annealed the crystal at 500 °C in the same atmosphere as employed in the first annealing procedure. We used Fourier spectroscopy for a photon energy range of 0.01–0.8 eV and grating spectroscopy for 0.6–32 eV. For the high-energy measurements (>6 eV), we utilized synchrotron radiation at the Institute for Molecular Science (UV-SOR) as a light source. The *T* dependence of the reflectivity was measured for 0.01–3 eV over the range of 10–540 K. The room-temperature data for above 3 eV were used to perform a Kramers-Kronig analysis and deduce optical-conductivity spectra at respective *T*. For the analysis, we assumed the Hagen-Rubens relation below 0.01 eV and ω^{-4} extrapolation above 32 eV. In Raman scattering measurements, a 514.5-nm line from an argon ion laser was used as the incident light. The backward-scattered light was collected and dispersed by a triple monochromator equipped with a liquid-nitrogen-cooled charge-coupled-device detector.

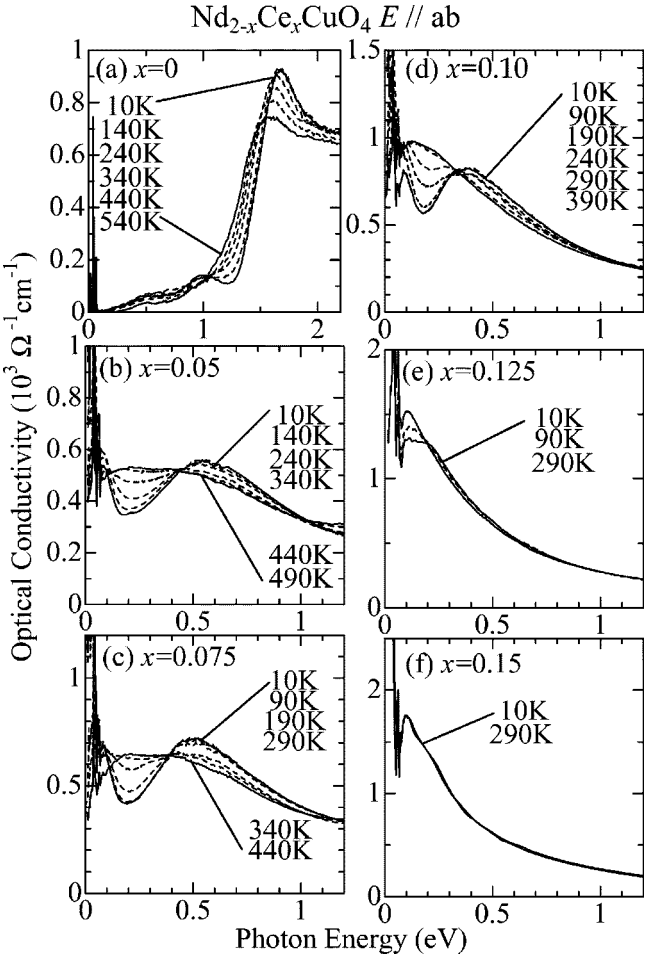

FIG. 3. Optical conductivity spectra at various temperatures for crystals of $Nd_{2-x}Ce_xCuO_4$ ($x=0$–0.15).

III. RESULTS AND DISCUSSION

A. Optical spectra: Pseudogap and related low-energy charge dynamics

We show in Fig. 1 the *T* variation of reflectivity spectra below 2.5 eV for crystals of $Nd_{2-x}Ce_xCuO_4$ ($x=0$–0.15). The reflectivity spectra of the undoped sample ($x=0$) are mainly composed of optical phonon modes and a broad peak at around 1.5 eV, which is due to the charge transfer (CT) excitation from O2*p*-like to Cu3*d*-like (upper Hubbard band) states. With Ce doping, the peak at 1.5 eV becomes broader, and alternatively a high-reflectivity band below 1 eV evolves as accompanied by the plasma edge at around 1.2 eV. For $x=0.15$, a higher reflectivity was reported by some groups,[28,29] which may be owing to a sight difference in the doping level. Because of this difference, the conductivity is somewhat lower and the scattering rate is higher and less steep than those of the literature[28,29] (see Figs. 2–6). In the underdoped region ($0.05\leqslant x\leqslant0.125$), the spectra show a relatively large *T* dependence while those for the $x=0.15$ crystal show little *T* variation. In the case of $x=0.10$, for example, a hollow structure evolves at around 0.3 eV and the reflectivity increases largely below 0.2 eV with decreasing *T*. Similar tendencies are observed, more or less, in the whole underdoped region ($0.05\leqslant x\leqslant0.125$). These structures are responsible for a pseudogap and Drude response in the optical conductivity spectra (see Figs. 2–4), respectively.

We plot in Fig. 2 the doping dependence of the optical conductivity spectra for the crystals of $Nd_{2-x}Ce_xCuO_4$ with $x=0$–0.15 below 2.2 eV at 10 K and also at the sufficient high *T* (440 K for the $x=0.05$, 290 K for the others). The spectra of the $x=0$ crystal show a broad peak around 1.5 eV due to the CT excitation, forming a gaplike structure. Figure 3(a) illustrates the *T* variation of optical conductivity spectra for the $x=0$ crystal. The peak of the CT excitation becomes sharper and the peak energy increases by 0.2 eV with decreasing *T* from 540 K to 10 K. Similar behaviors of the spectra for the parent compounds of the high-T_c cuprate were already reported in the literature,[30,31] in which these *T*-dependent features have been interpreted as due to electron-phonon coupling[30] or antiferromagnetic correlation.[31]

As shown in Fig. 2, the intensity of the CT excitation decreases with Ce doping, and alternatively the spectral weight of intraband excitation below 1 eV increases. At high *T* (dashed lines), the spectrum of the $x=0.05$ crystal shows a flat shape below 0.5 eV, being far from that of the Drude response. With further doping, the spectral weight tends to be accumulated in the lower-energy region, forming a Drude-like peak at $\omega=0$. These behaviors have already been reported by previous studies[32,33] and are common to those of the hole-doped cuprates[34] and other filling-control Mott transition systems.[35] While the spectra for the superconducting $x=0.15$ crystal show little *T* variation, for the underdoped crystals ($x=0.05$, 0.10, 0.125) the spectral weight at around 0.2 eV decreases when the *T* is lowered down to 10 K. To examine these behaviors in more detail, we show the *T* dependence of optical conductivity spectra for the crystals with $x=0.05$–0.15 in Figs. 3(b)–3(f). In the case of the $x=0.10$

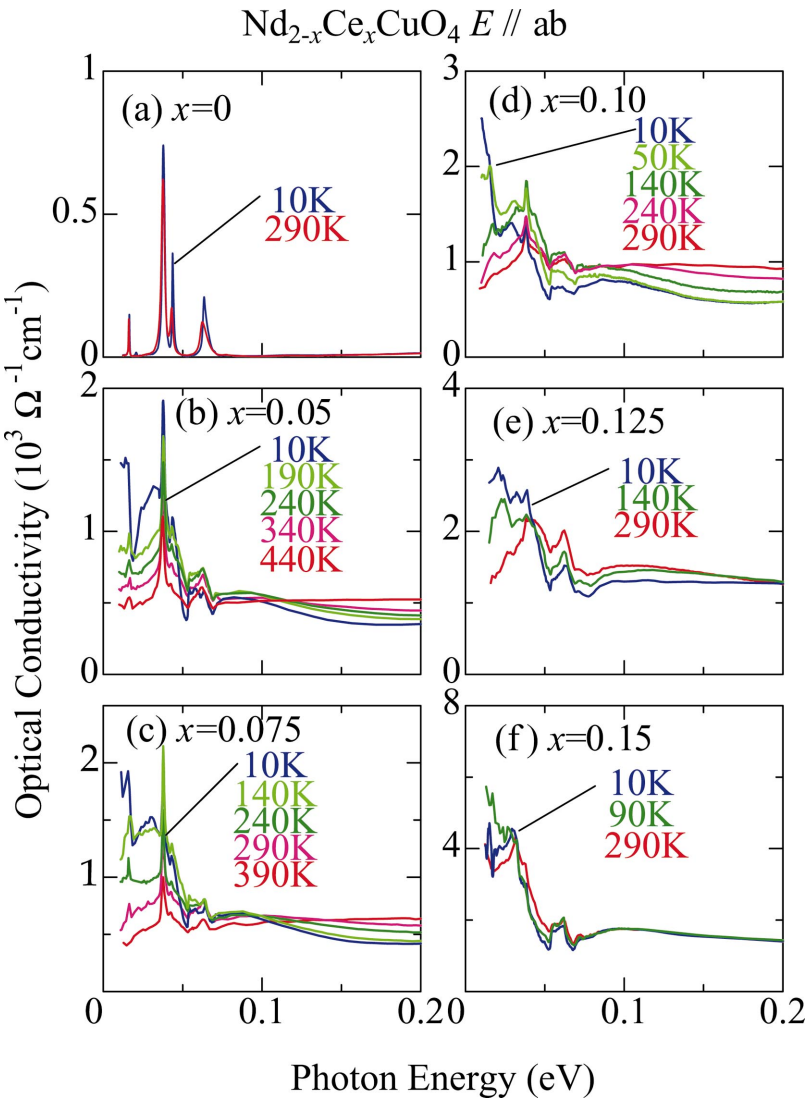

FIG. 4. (Color) Low-energy part (≤ 0.2 eV) of the optical conductivity spectra at various temperatures for crystals of $Nd_{2-x}Ce_xCuO_4$ ($x = 0-0.15$).

crystal, for example, the spectral weight at around 0.2 eV decreases with decreasing T from 290 K while the spectra show little T variation above 290 K. At low T, the spectral shape shows a gaplike structure on an energy scale as large as 0.3 eV. In the lower-energy region below 0.15 eV the conductivity increases toward lower energy, which corresponds to the tail of the Drude response (see also Figs. 4 and 6). The notable pseudogap formation is observed in the whole underdoped region ($x < 0.15$). The magnitude of the pseudogap may be measured by the energy of the isosbetic (equal-absorption) point in the course of the spectral weight transfer. The isosbetic point energy decreases from 0.43 eV to 0.17 eV with increasing Ce concentration from $x = 0.05$ to $x = 0.125$. It is worth noting that the energy is of the same order as that of the antiferromagnetic spin exchange interaction (≈ 0.12 eV).[36,37] Such a distinct pseudogap formation has never been observed in the bare optical spectra of the hole-underdoped cuprates, in which the ground state is superconducting and is different from that in the underdoped $Nd_{2-x}Ce_xCuO_4$.[38]

Figure 4 illustrates the T variation of the optical conductivity spectra below 0.2 eV for $Nd_{2-x}Ce_xCuO_4$ with various Ce concentrations. Structures related to optical phonons are clearly discerned in this region. Four phonon modes are observed in the spectra of the $x = 0$ crystal, which is consistent with factor group analysis. These phonon modes can be assigned to the Cu-O stretching mode (0.063 eV), Cu-O bending mode (0.043 eV), the vibration of Nd-O (external mode) in the block layer (0.037 eV), and the vibration between the CuO_2 layer and the block layer (0.016 eV).[39] While the external mode (0.037 eV) can hardly couple with electrons and in fact decreases in intensity with electron doping, dip structures emerge at around the energies of the other phonon modes in the spectra of the doped crystals, especially at low T. These are typical of Fano antiresonance induced by the interaction between a boson mode and electronic continuum.[42] Such an electron-boson coupling is known to manifest itself as a kink of scattering rate spectra $1/\tau(\omega)$ at around the energy of the boson mode.[43] We show the $1/\tau(\omega)$ and $m^*(\omega)/m_0$ spectra at 10 K for the crystals with $x = 0.10$, 0.125, and 0.15 in Fig. 5. The $1/\tau(\omega)$ and $m^*(\omega)/m_0$ are given in terms of the extended Drude formula,

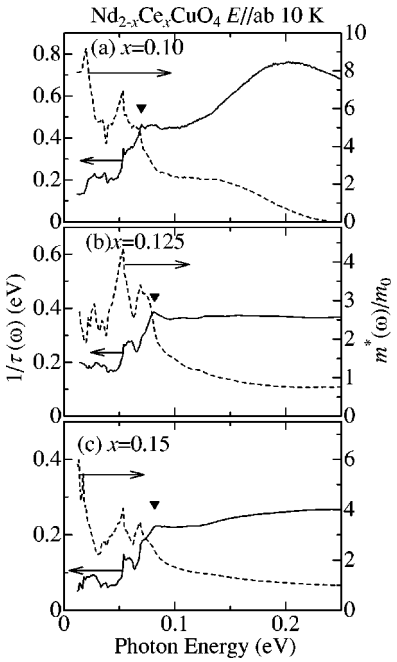

FIG. 5. Scattering rate spectra $[1/\tau(\omega)]$ and effective mass spectra $[m^*(\omega)/m_0]$ below 0.25 eV at 10 K for crystals of $Nd_{2-x}Ce_xCuO_4$ with $x=0.10$, 0.125, and 0.15.

$$\frac{1}{\tau(\omega)} = \frac{\omega_p^2}{4\pi}\mathrm{Re}\left(\frac{1}{\tilde{\sigma}(\omega)}\right), \tag{1}$$

$$\frac{m^*(\omega)}{m_0} = \frac{\omega_p^2}{4\pi\omega}\mathrm{Im}\left(\frac{1}{\tilde{\sigma}(\omega)}\right), \tag{2}$$

where ω_p, $\tilde{\sigma}(\omega)$, and m_0 are plasma frequency, complex conductivity, and bare electron mass, respectively. We obtained the plasma frequency by integration of the optical conductivity up to 1.2 eV. In the $1/\tau(\omega)$ spectrum of the $x=0.10$ crystal, a broad peak is discerned at around 0.2 eV, which is owing to the pseudogap formation. (The anomaly of the m^*/m_0 spectrum above 0.15 eV is also an artifact due to the pseudogap feature.) These features are hardly observed in the spectra of $x=0.125$ and $x=0.15$ consistent with the weak pseudogap feature in these compound. In the lower-energy region, kinks are observed at around 0.07 eV in the $1/\tau(\omega)$ spectra of all the crystal ($x=0.10$–0.15) as indicated by symbols (solid triangles). Correspondingly, $m^*(\omega)/m_0$ is enhanced below 0.07 eV. Recently, a similar kink in the scattering rate was reported by Singley *et al.*, who considered the kink as an indication of pseudogap formation.[28] The energy of the kink in the scattering rate spectra almost corresponds to the energy of the highest-lying dip structure in the optical conductivity spectra. In general, a dip in the optical conductivity and a kink in the scattering rate spectrum are expected when strong coupling is considered between electrons and a boson mode. A magnetic mode strongly coupled to electronic continuum might be a possible origin of the kink in the scattering rate spectra. In the present case, however, the kink structure for the antiferromagnetic $x=0.10$ crystal is quite similar to that for the superconducting $x=0.15$ crystal. Therefore, the observed kink structure can hardly be ascribed to the magnetic mode although a complete mapping of the spin excitations must be needed to make a final statement. Alternatively, we ascribed the boson mode to the optical phonon mode because the energy of the kink shows no Ce concentration dependence and is in accordance with that of optical phonon (Cu-O stretching mode). The kink structure observed in the scattering rate spectra is likely relevant to the kink structure in the ARPES spectra, which is observed not only in the electron-doped system but also in the hole-doped system.[44–47]

Next, we focus on the genuinely electronic structure in the low-energy region, apart from the structures related to the optical phonon. As shown in Fig. 4, the spectral weight below 0.03 eV increases with decreasing T in the spectra for the underdoped crystals, while the spectra for the $x=0.15$ crystal undergo a minimal change. To compare the evolution of the low-energy spectral weight and the pseudogap formation in the underdoped region, we show in Fig. 6 the optical conductivity spectra (0.01–2.5 eV) of the crystals with $x=0$–0.15 on a logarithmic scale. First, let us discuss the spectra for the $x=0.10$ crystal as an example. Above 290 K where the pseudogap structure is not observed, the spectra show almost flat shape below 0.4 eV. With decreasing T from 290 K, the spectral weight below 0.03 eV evolves concomitantly with the pseudogap formation. At low T the conductivity steeply increases toward $\omega\sim 0$ as an indication of Drude response. Similar behaviors are, more or less, observed in all the underdoped crystals ($x=0.05$–0.125).

To discuss a more quantitative aspect, we in Figs. 7(a)–7(e) plot the spectral weight below 0.03 eV [region *A* in Fig. 7(f)] as a measure of the Drude response as well as the change in spectral weight (ΔN_{eff}) from at 540 K between 0.12 eV and the isosbectic point [region *B* in Fig. 7(f)] as a measure of pseudogap formation. Both quantities are deduced from the calculated effective number of electrons N_{eff} defined by the following relation:

$$N_{\mathrm{eff}}(\omega) = \frac{2m}{\pi e^2 N}\int_0^{\omega}\sigma(\omega')d\omega', \tag{3}$$

where N represents the number of formula units per unit volume. The ΔN_{eff} of the underdoped crystals begins to increase rapidly at around the T indicated by an arrow, which defines the onset T of the pseudogap (T^*). The N_{eff} at 0.03 eV also begins to increase rapidly at around T^* for the crystals of $x=0.05$, 0.075, 0.10. This clearly shows that the Drude response evolves concomitantly with pseudogap formation. Such a feature becomes less clear but is still discerned for the $x=0.125$ crystal. The N_{eff} at 0.03 eV monotonically increases towards low T due to the sharpening of the Drude-like response in the case of $x=0.15$ crystal.

We plot the T^* in Fig. 8(c) as a function of x together with Néel temperature (T_N) reported by Luke *et al.*[19] We also plot the magnitude of the pseudogap (Δ_{PG}) defined by the energy of the isosbectic point in Fig. 8(b). Both the Δ_{PG} and T^* decrease with electron doping. The ratio of Δ_{PG} to k_BT^* is ≈ 10 throughout the underdoped region. The doping variations of the spectral weight below 0.03 eV at 10 K and

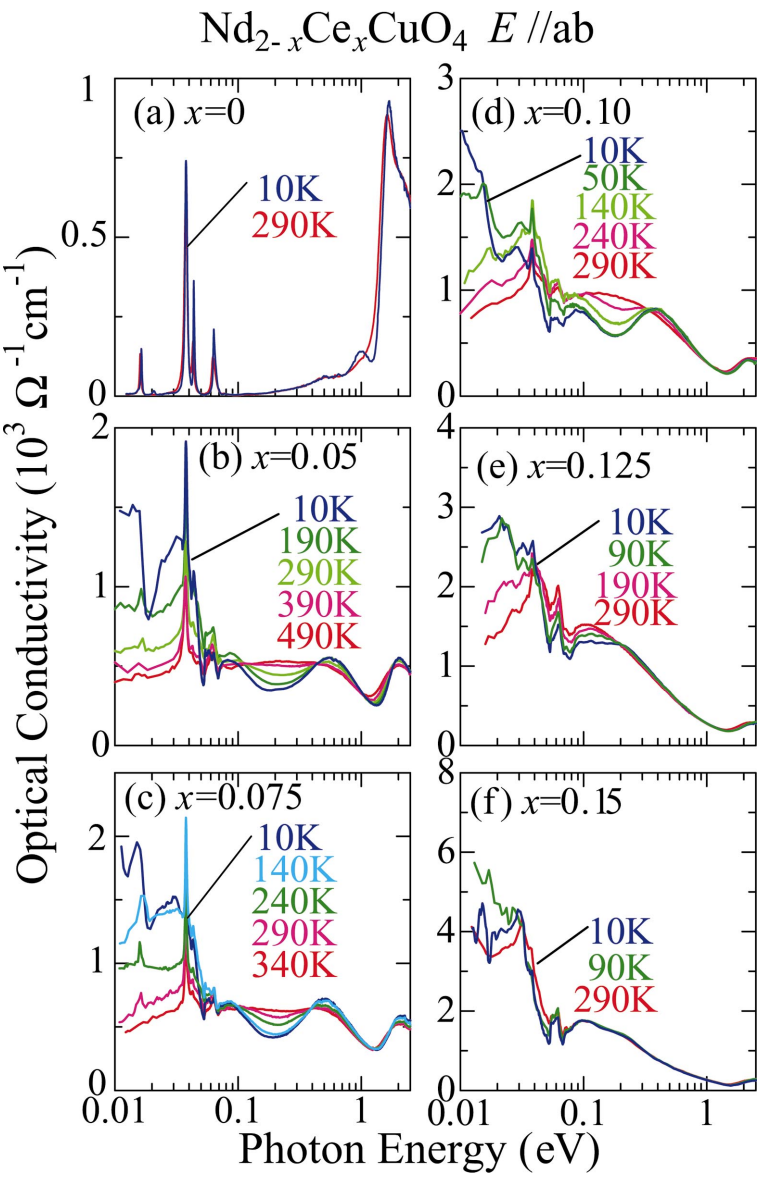

FIG. 6. (Color) Temperature dependence of the optical conductivity spectra for crystals of $Nd_{2-x}Ce_xCuO_4$ ($x=0-0.15$) on a logarithmic scale of photon energy.

540 K are shown in Fig. 8(a) together with that of the intraband excitation ($\leqslant 1.2$ eV) at 10 K. As already reported in the literature,[32,33] the spectral weight of the intraband excitation increases largely with doping at first and then saturated. On the other hand, the low-energy spectral weight below 0.03 eV in the underdoped region is much suppressed as compared with the case of $x=0.15$. Especially, in a high-T region (e.g., at 540 K) the low-energy spectral weight is very small, signaling the incoherent nature of charge transport at high T ($T>T^*$). When T is lowered down to 10 K, a sharp Drude-like component emerges even in the underdoped region. Thus, the spectral weight below 0.03 eV represents the Drude weight at least at such a low T. As seen in Fig. 8(a), the Drude-like weight increases linearly with electron doping in the underdoped region ($x<0.15$), while for $x=0.15$ it is much larger than that expected by this linear relation. All the features concerning the doping dependence of the Drude-like weight are even quantitatively similar to those observed in $La_{2-x}Sr_xCuO_4$.[34,48] A similar electron-hole symmetric behavior was also observed in the nominal carrier number obtained by Hall coefficient.[9,10,23,49]

B. Influence of pseudogap formation on transport properties

We show the T variation of in-plane resistivity for the crystal with various Ce concentrations ($x=0-0.15$) in Fig. 9(a). The resistivity of the parent compound ($x=0$) shows an insulating behavior in the whole T region. On the other hand, the resistivity for the $x=0.15$ crystal shows a metallic behavior from 600 K to 25 K ($=T_c$). In the underdoped region ($x=0.025-0.125$), the resistivity shows a barely metallic behavior at high T but an upturn at low T. To discuss the behavior of the resistivity in detail, we plot the resistivity normalized by the value at 600 K [$\rho(T)/\rho(600\ \mathrm{K})$] in Fig.

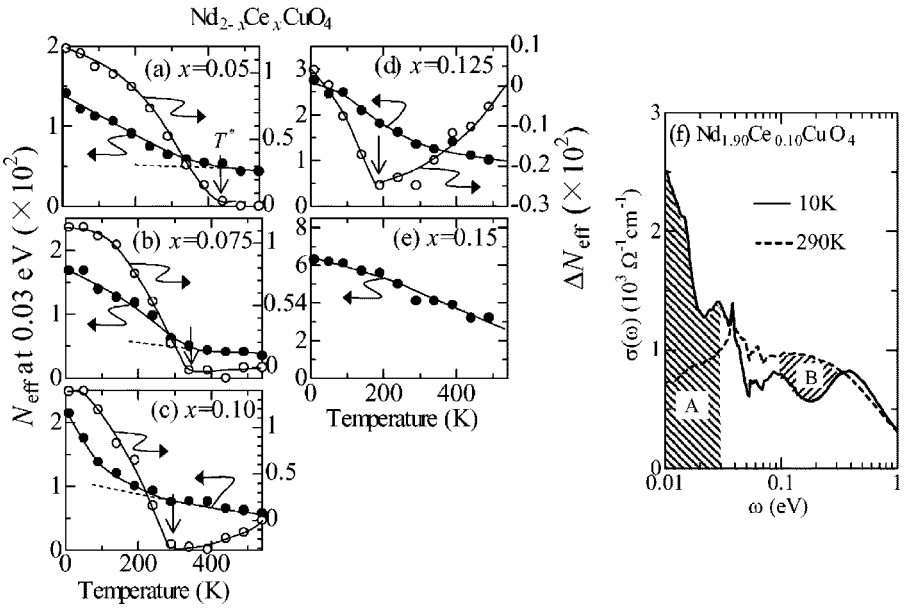

FIG. 7. (a)–(e) The temperature variation of the effective number of electrons, N_{eff}, at 0.03 eV [solid circles, *A* region in (f)] and of the loss of the spectral weight (ΔN_{eff}) due to the formation of pseudogaps [open circles, *B* region in (f)] for crystals of $Nd_{2-x}Ce_xCuO_4$ ($x=0.05$–0.15). Solid lines are merely a guide to the eyes. (f) The optical conductivity spectra of the $x=0.10$ crystal at 10 K and 290 K. The hatched region *A* stands for the spectral weight below 0.03 eV and the hatched region *B* indicates the spectral weight loss due to pseudogap formation (ΔN_{eff}).

9(b). The resistivity for the $x=0.15$ crystal can be fitted by the relation $\rho=aT^2+\rho_0$, between 25 K and 200 K as reported previously.[50] Above 200 K, the power becomes slightly lower (≈ 1.6). The power in the resistivity of the $x=0.10$ and 0.125 crystals above 300 K is also 1.5–1.7. The *T*-linear behavior in resistivity is not observed in any *T* and doping regions of the present study in contrast with the hole-doped case. The resistivity for $x=0.10$ and 0.125 shows an upturn at low *T* (50–100 K), which may be due to the weak localization effect.[51,52] The influence of the localization is not observed in the optical spectra of these crystals such as a decrease of the conductivity above 0.01 eV, indicating that the localization is restricted to the fairly low-energy scale (<0.01 eV). For the crystal with the lower doping level ($x<0.10$), some change is observed in the resistivity behavior at relatively high *T* (300–600 K). The resistivity for $x=0.05$ and $x=0.075$ tends to saturate toward higher *T* ($d^2\rho/dT^2<0$). For $x=0.025$, the resistivity is no more metallic, i.e., $d\rho/dT<0$, above 430 K. Importantly, the resistivity for the crystal with $x=0.025$–0.075 begins to decrease rapidly at around the *T* marked by symbols (solid triangles), although the resistivity of these crystal also shows upturn at around 100–150 K due to the weak localization effect. The *T* marked by the symbols almost coincide with T^* below which the pseudogap begins to evolve in the optical spectra. Moreover, the steep decrease of resistivity below T^* is consistent with the evolution of Drude-like response. Therefore, we have concluded that the anomalies in the resistivity are caused by the pseudogap formation. It is worth noting that similar behaviors are also observed in the hole-doped cuprates, which have been assigned to being a consequence of pseudogap formation.[53,54]

Even a clearer anomaly due to pseudogap formation is observed in the out-of-plane transport. We show the *T* variation of the out-of-plane resistivity in Fig. 10(a) and the ratio of the out-of-plane resistivity to the in-plane resistivity (ρ_c/ρ_{ab}) in Fig. 11. The out-of-plane resistivity (along the *c* axis) shows a much higher value than the in-plane resistivity ($\rho_c/\rho_{ab}\sim 10^3$–$10^5$), reflecting a strong two-dimensional nature of the charge dynamics in $Nd_{2-x}Ce_xCuO_4$ with the T' structure where no apical oxygen is present. Such a strong two dimensionality also gives raise to an increase of ρ_c/ρ_{ab} toward low *T* in the high-*T* region for all crystals. While the out-of-plane resistivity of the $x=0.15$ crystal is metallic ($d\rho_c/dT>0$) in the whole *T* region we measured, that of the underdoped region shows a complex behavior. For example, the resistivity of the $x=0.075$ crystal increases with decreasing *T* in the high-*T* region above 300 K. The increase in the resistivity saturates at around 360 K and then the resistivity decreases below the 300 K. At around 100 K, the resistivity shows an upturn again, probably due to the localization effect. A similar behavior is observed in all the underdoped crystals. To obtain the onset *T* of the decrease in the out-of-plane resistivity, we plot the *T* derivative of the resistivity ($d\rho_c/dT$) in Figs. 10(b)–10(f). Reflecting the decrease of resistivity, $d\rho_c/dT$ increases at around the *T* indicated by arrows (T_ρ). To be strict, the T_ρ corresponds to the *T* where the increase in the resistivity tends to saturate (e.g., 360 K for the $x=0.075$ crystal). We show the T_ρ for the respective crystals in Fig. 8(c). The T_ρ almost coincides with the T^* obtained by the analysis of optical conductivity spectra. This suggests that the decrease in the out-of-plane resistivity is also induced by pseudogap formation. Because the decrease is much more significant than that in the in-plane resistivity,

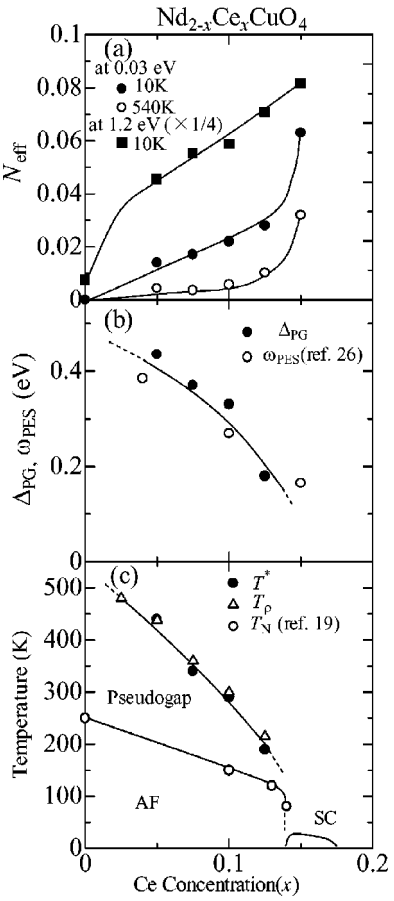

FIG. 8. (a): The x variation of N_{eff} at 0.03 eV at 10 K and 540 K (solid and open circles, respectively) and at 1.2 eV and 10 K (solid squares). (b) The x variation of the pseudogap magnitude Δ_{PG} as defined by the higher-lying isosbetic (equal-absorption) point in the temperature-dependent conductivity spectra and the magnitude of the pseudogap (ω_{PES}) in the photoemission spectra (Ref. 26). The ω_{PES} is defined as the maximum energy of the quasiparticle peak on the putative large Fermi surface in the ARPES spectra shown in the Figs. 2(c)–(e) of Ref. 26. (c) The obtained phase diagram of $Nd_{2-x}Ce_xCuO_4$. The onset temperature of pseudogap formation (T^*) and the crossover temperature of out-of-plane resistivity (T_ρ) are plotted against x together with the Néel temperature T_{N} reported previously by Luke *et al.* (Ref. 19). Solid and dashed lines in (a)–(c) are merely a guide for the eyes.

the ρ_c/ρ_{ab} decreases with decreasing T in the low-T region for the underdoped crystals as shown in Fig. 11. The sensitivity of these transport characteristics to pseudogap formation is accounted for in the following arguments.

C. Comparison with angle-resolved photoemission spectra

Recently, angle-resolved photoemission spectroscopy on the $Nd_{2-x}Ce_xCuO_4$ including the underdoped region was performed by Armitage *et al.*[24–26] In the spectra of the underdoped region ($x=0.04$ and 0.10), a pseudogap is observed at around $(\pi/2,\pi/2)$ in the two-dimensional k space, while a small electron pocket or *Fermi arc* is observed at around $(\pi,0)$. This behavior is contrastive with the hole-doped case where pseudogap formation is observed at

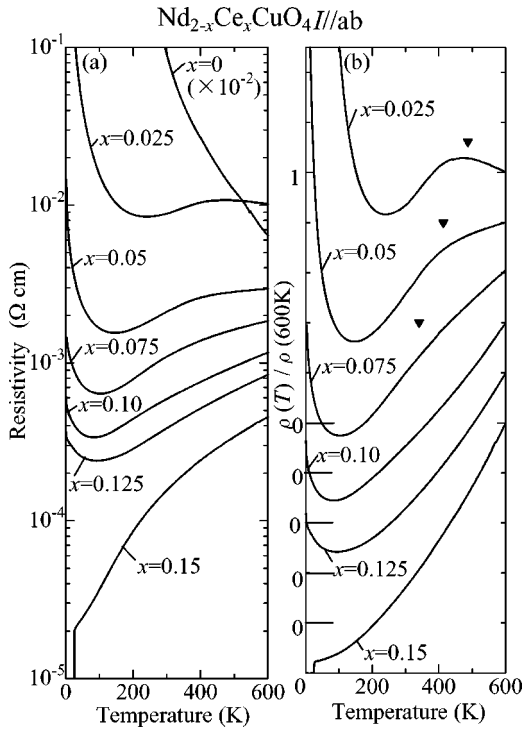

FIG. 9. (a) The T variation of the in-plane resistivity of the $Nd_{2-x}Ce_xCuO_4$ crystals with various x. (b) The T variation of the in-plane resistivity normalized by its 600 K value.

around $(\pi,0)$ and the Fermi arc at around $(\pi/2,\pi/2)$ in the underdoped region.[2,6,7] To compare the magnitude of pseudogap in the ARPES spectra with that appearing in the optical spectra, we plot the magnitude of the pseudogap ω_{PES}

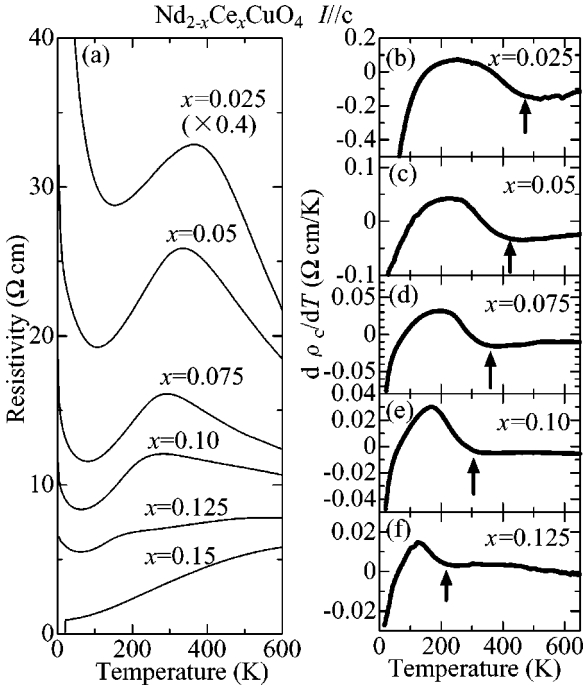

FIG. 10. (a) The T variation of the out-of-plane resistivity of the $Nd_{2-x}Ce_xCuO_4$ crystals with various x. (b)–(f) The temperature derivative of the out-of-plane resistivity ($d\rho_c/dT$).

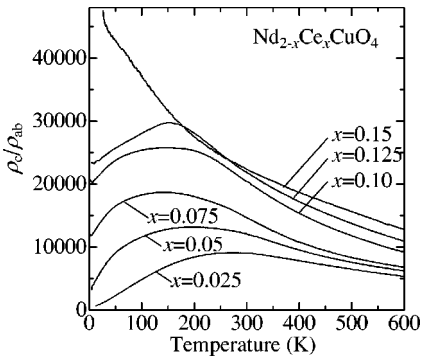

FIG. 11. The T variation of the ratio of the out-of-plane resistivity to the in-plane resistivity (ρ_c/ρ_{ab}) for $Nd_{2-x}Ce_xCuO_4$ crystals with various x.

in the ARPES spectra (for the definition, see the figure caption) together with the Δ_{PG} in Fig. 8(b). It is clear from this figure that the energy scale of the pseudogap emerging in the ARPES spectra is comparable with that in the optical spectra. Moreover, the small Drude weight ($\propto n/m^*$) proportional to x is also consistent with the existence of the electron pocket feature if the effective mass does not show a strong doping variation. This is supported by the fact that the nominal carrier number per Cu obtained by the Hall coefficient at a low T almost coincides with x in the underdoped region.[23,55] Therefore, the pseudogap in the optical conductivity spectra corresponds to that in ARPES spectra at around $(\pi/2,\pi/2)$ and the Drude response to the carriers at around $(\pi,0)$. As for the pseudogap behavior of the $x=0.15$ crystal, however, the optical spectra are not well consistent with the ARPES spectra. The pseudogap is not discerned in the optical spectra while in the ARPES spectra a pseudogap has been observed at the cross section of the antiferromagnetic Brillouin zone boundary and the (large) Fermi surface for the crystal with $x=0.15$. This is perhaps because the measure of the k space where the pseudogap is present for $x=0.15$ is too small to be observed in the optical conductivity spectrum, which is the average of the charge response over the whole k space.[56]

Figure 12 schematically illustrates the T and doping evolution of the Fermi surface we propose here based on the results of optical and photoemission spectra. There are the pseudogap at around $(\pi/2,\pi/2)$ and the small electron pocket (or Fermi arc) at around $(\pi,0)$ at low T in the underdoped region as observed in the ARPES spectra. The magnitude of the pseudogap decreases with doping. In the sufficiently overdoped region, a large Fermi surface is expected. As discussed above, the pseudogap at around $(\pi/2,\pi/2)$ in the underdoped region can also be observed in the optical spectra. The pseudogap gradually closes with increasing T in optical spectra of the underdoped region. In the high-T region ($T>T^*$), the pseudogap feature is not discerned at all. This result indicates that the large Fermi surface is revived above T^* even in the underdoped region.

Transport properties are strongly affected by the crossover between the small Fermi surface at low T and the large Fermi surface at high T in the underdoped region. One such example is the Hall coefficient. As we reported previously,[23] the absolute value of the Hall coefficient tends to increase rapidly at around T^* where the pseudogap begins to be formed. This is consistent with the present scenario—namely, that T^* is the onset of the crossover from the large to small Fermi surface. The other example is the out-of-plane resistivity. As described above, the resistivity decreases rapidly at around T^*. By contrast, the out-of-plane resistivity of the hole-doped cuprate *increases* rapidly at around the T below which the pseudogap opens.[57] One of the plausible scenarios to explain such an anomaly in the hole-doped system is that the interplane charge transport is dominated by the carriers at around $(\pi,0)$ and hence that the out-of-plane resistivity increases in the course of pseudogap formation at around $(\pi,0)$.[58] Therefore, the contrastive behaviors of the out-of-plane resistivity in the electron-doped versus hole-doped cuprates as observed can be ascribed to the difference of the k position of the pseudogap. In the electron-doped system, pseudogap formation at around $(\pi/2,\pi/2)$ is expected to hardly affect the out-of-plane charge transport, which is sensitive to $(\pi,0)$. On the other hand, the electronic state at the rest part of Fermi surface—namely, around $(\pi,0)$—becomes coherent below T^* as indicated by the evolution of the Drude response. Such a formation of the coherent carriers (quasiparticles) around the $(\pi,0)$ point can explain the observed enhancement of the out-of-plane transport below T^*. These results also ensure that the pseudogap appearing below T^* in the optical conductivity is identical with the pseudogap at around $(\pi/2,\pi/2)$ observed in the ARPES spectra.

D. Origin of the pseudogap

We previously proposed the possibility of charge ordering as the origin of the large pseudogap in the as-grown (or

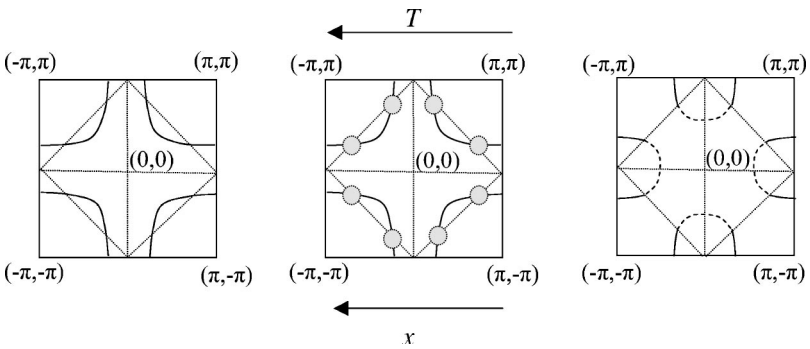

FIG. 12. Schematic illustration of the temperature (T) and doping (x) variations of the Fermi surface. Solid lines stand for the Fermi surface. Dotted lines connecting $(\pm\pi,0)$ and $(0,\pm\pi)$ indicate the magnetic Brillioin zone in the case of (π,π) spin ordering. Arrows show the increasing direction of T and x.

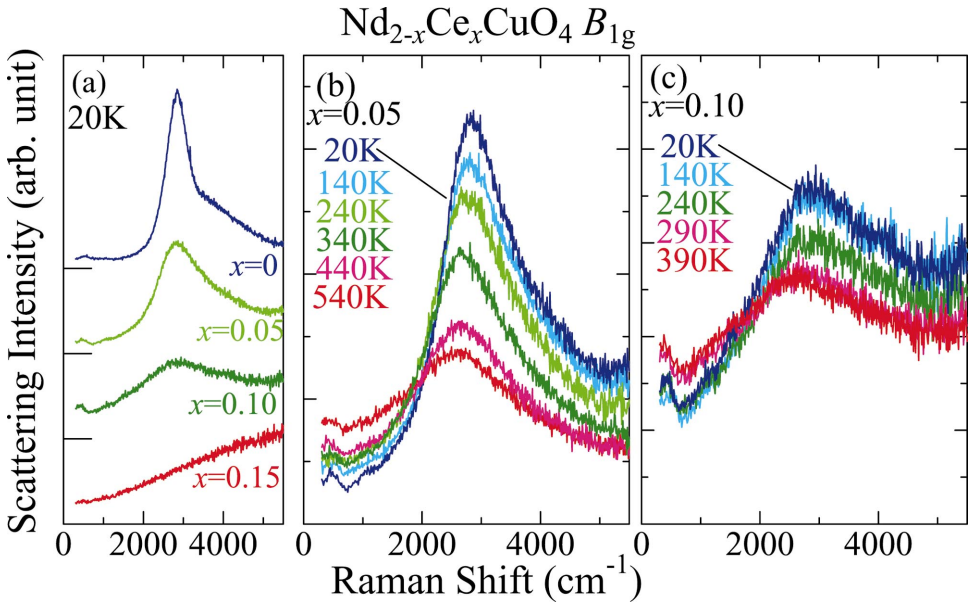

FIG. 13. (Color) (a) Doping variation of B_{1g} Raman spectra (two-magnon scattering) at 20 K for crystals of $Nd_{2-x}Ce_xCuO_4$ ($0 \leqslant x \leqslant 0.15$). (b),(c) Temperature variation of B_{1g} Raman spectra for (b) $x=0.05$ and (c) $x=0.10$ crystals.

oxygenated) crystal,[22] which is thought to be essentially the same as that in the underdoped reduced crystal. However, the possibility of stripe order contradicts with the (π,π) spin order of $Nd_{2-x}Ce_xCuO_4$ ($x<0.15$) as recently observed in the neutron diffraction measurement.[59] Apart from the vertical (metallic) stripe order, the concomitant evolution of a Drude-like response with the pseudogap cannot be explained by the usual (insulating) charge-ordering scenario. The possibility of electronic phase separation into the insulating antiferromagnetic state and the metallic state is also denied as the origin of the pseudogap. Although some crystals in this system show phase coexistence, this is restricted to a very narrow doping range near the antiferromagnetic-superconducting phase boundary.[60,61] In addition, the *k*-dependent feature of the pseudogap cannot explained by the simple phase separation picture. In the case of the preformed pair, the pseudogap should be comparable in magnitude with the superconducting gap. In the present system, however, the magnitude of the superconducting gap is about 5 meV.[24,46] Alternatively, we propose here that the origin is the antiferromagnetic spin correlation. There are several experimental evidences for this: (a) In the underdoped region where the pseudogap is observed, long-range antiferromagnetic order emerges [see Fig. 8(c)] in further decreasing T below T^*. (b) The antiferromagnetic interaction (J) is as large as the energy scale of pseudogap.[36,37] (c) The strong *k*-space anisotropy of the pseudogap as observed by ARPES coincides, at least qualitatively, with that expected for the antiferromagnetic or spin-density-wave (SDW) gap.[62] A high onset T of the pseudogap ($T^* \approx 2T_N$) compared with Néel temperature (T_N) can be reasonably ascribed to the two-dimensional nature of spin correlation in the present system. Then, another question to be answered is why Drude response evolves below T^*—i.e., the onset of the strong antiferromagnetic correlation. Our interpretation is that the evolution of the Drude response is due to a decrease of spin scattering in the course of the increase of antiferromagnetic correlation. Then, the question may be why the evolution of the Drude response begins at T^* rather than at T_N. In the present system with strong two-dimensional (2D) nature, the strong in-plane antiferromagnetic spin correlation is expected to well develop even above T_N. In fact, the antiferromagnetic spin correlation length ξ of the underdoped crystal was observed to be longer than $5a$ (a, in-plane lattice constant) even at 100 K above T_N.[63] On the other hand, the carrier mean free path l in the underdoped region is not so large as ξ at around T^*. In the Boltzmann transport theory, resistivity in a 2D system is given as

$$\rho = \frac{hd}{e^2}\frac{1}{k_F l}, \tag{4}$$

where d stands for interplane distance. Since the large Fermi surface must satisfy the Luttinger theorem, k_F is given as $\sqrt{2(1-x)}\pi/a$ in this simplified 2D model. This value is in accordance with the result of the ARPES experiment.[24,25]

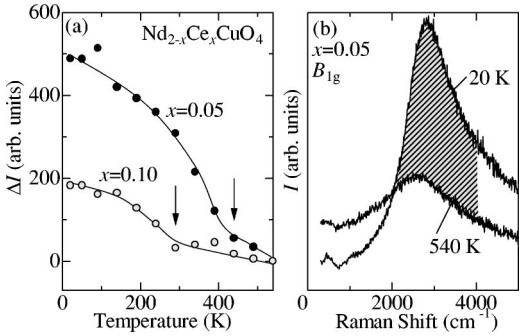

FIG. 14. (a) The T variation of the intensity of the two-magnon band for $x=0.05$ and 0.10 crystals as estimated by the change in the integrated scattering intensity of B_{1g} Raman spectra from 540 K between 2000 cm^{-1} and 4000 cm^{-1}. Solid lines are merely a guide to the eyes. (b) B_{1g} Raman spectra of the $x=0.05$ crystal at 20 K and 540 K. The hatched region stands for the change in intensity of the two-magnon peak as plotted in (a).

Putting the observed ρ values into Eq. (3), we obtain the l values at $T^* \approx 1.00a$ and $\approx 2.42a$ for the $x=0.10$ and 0.125 crystals, respectively.[64] The relation that $\xi > l$ well holds near below T^* in the underdoped region. In this case, the spin scattering of electron is expected to decrease with increasing antiferromagnetic correlation. This explanation is also supported by the fact that the evolution of the Drude response and the decrease of in-plane resistivity are more clearly observed in the lower-doped crystal where the larger change in spin scattering is anticipated.

Another piece of supporting evidence for the antiferromagnetic correlation scenario can be obtained from the T dependence of two-magnon Raman scattering spectra. We show the doping variation of the B_{1g} Raman scattering spectra for the $Nd_{2-x}Ce_xCuO_4$ crystals ($0 \leqslant x \leqslant 0.15$) at 20 K in Fig. 13(a). As reported previously, a two-magnon peak is clearly observed at around 2800 cm^{-1} in the spectrum of the $x=0$ crystal.[36] The two-magnon peak becomes broader and its intensity decreases with Ce doping while the peak energy shows little doping dependence.[65] In the spectrum for the $x=0.15$ crystal, the two-magnon peak is not discerned. This peak shows a strong T variation in the spectra of the underdoped crystal. In Fig. 13(b), we exemplify the T variation of the B_{1g} Raman scattering spectra for the $x=0.05$ crystal. The intensity of the two-magnon peak decreases with increasing T from 20 K, signaling the decrease of antiferromagnetic correlation. At 540 K, the peak still remains but the intensity is much reduced from the one at the low T. A similar tendency is observed in the spectra of the $x=0.10$ crystal as shown in Fig. 13(c), although the peak shape is broader than that for the $x=0.05$ crystal. As the measure of the two-magnon band intensity, we estimated the change [ΔI, hatched region in Fig. 14(b)] of the integrated intensity of the B_{1g} Raman scattering spectra between 2000 cm^{-1} and 4000 cm^{-1} from the one at 540 K. The T dependence of ΔI is shown for the $x=0.05$ and $x=0.10$ crystals in Fig. 14(a). Importantly, the ΔI for the both crystals increases rapidly at around T^* indicated by arrows with decreasing T. This suggests that the antiferromagnetic spin correlation steeply evolves below T^* in the underdoped region. This is quite consistent with the present conclusion about the origin of the pseudogap.

E. Comparison with the hole-doped case

The smaller pseudogap in hole-doped cuprates is of the order of the superconducting gap and is clearly distinct in nature from the large-energy pseudogap in electron-doped system. The energy scale of the large-energy pseudogap in the hole-doped system is as large as several hundreds meV, similar to the present electron-doped system. In addition, the large-energy pseudogap in both electron- and hole-doped systems governs the T-dependent large-to-small crossover of the Hall coefficient, of which the T and doping dependences of the absolute value are confirmed to be almost identical.[9] However, there are several differences between both pseudogaps. (a) The large-energy pseudogap of the hole-doped system is observed at around $(\pi,0)$ in contrast with that at around $(\pi/2,\pi/2)$ of the electron-doped cuprate. (b) The pseudogap feature is not discerned in the optical conductivity spectra of the hole doped cuprate. (This may be simply because the gaplike feature in the hole-doped system is weaker than that in the electron-doped compound.) (c) The ground state in the underdoped region of electron-doped system, where the pseudogap formation is observed, is the antiferromagnetic state, while the superconducting phase is present even in the underdoped region for the hole-doped cuprate.

All these contrastive features may be explained in terms of the difference in the sign of the long-range hopping terms, t' and t'', in the respective systems.[66] Recent t-t'-t''-J model calculations suggest that the electrons doped into the parent insulator exist at around $(\pi,0)$, which is consistent with the observation of electron-pocket-like feature at around $(\pi,0)$ in the underdoped region of electron-doped cuprates, and that the antiferromagnetic correlation does not conflict with the charge transport of the electrons at around $(\pi,0)$.[66] So the antiferromagnetic correlation in the electron-doped system is stronger than that in the hole-doped system, which gives rise to notable pseudogap formation in the electron-doped system as observed also in the optical conductivity spectrum. While it is thus strongly suggested experimentally and theoretically that pseudogap formation in the electron-doped system is due to the antiferromagnetic correlation, in the hole-doped compound there have been proposed several possible scenarios to explain large-energy pseudogap formation, not only antiferromagnetic correlation[67] but also spin-charge separation,[68] stripe formation,[69] etc. At present, it is premature to conclude that the origin of the pseudogap in the hole-doped cuprate is identical to that in the electron-doped system—i.e., the antiferromagnetic spin correlation. However, even if not, quite a parallel behavior of the Hall coefficient correlated with pseudogap formation in the electron- and hole-doped systems needs to be explained.

IV. SUMMARY

We have measured the T and doping variations of the optical conductivity spectra for the crystals of $Nd_{2-x}Ce_xCuO_4$ ($0 \leqslant x \leqslant 0.15$). A pseudogap as large as 0.2–0.4 eV evolves concomitantly with the Drude-like response in the optical conductivity spectra of the underdoped crystals of $Nd_{2-x}Ce_xCuO_4$. The onset T (T^*) of the pseudogap decreases with electron doping toward the onset of the superconducting phase ($x \approx 0.14$). The magnitude (Δ_{PG}) of the pseudogap in the optical spectra, which is comparable to that observed in the photoemission spectra,[26] also decreases with x, while holding the relation that $\Delta_{PG} \approx 10 k_B T^*$. The scattering rate spectra $1/\tau(\omega)$ for the $x=0.10$–0.15 crystals show kinks at around 0.07 eV. We have ascribed them not to the pseudogap but to the electron-phonon coupling. We have also investigated the T and doping variations of both in-plane and out-of-plane resistivities for the crystals of $Nd_{2-x}Ce_xCuO_4$ ($0 \leqslant x \leqslant 0.15$). The in-plane resistivity in the underdoped region begins to decrease rapidly at around T^* in decreasing T, which is consistent with the evolution of the Drude response. The out-of-plane resistivity in the underdoped region begins to decrease even more rapidly below

T^*. The interplane transport in high-T_c cuprates is dominated by electronic states at around $(\pi,0)$. Therefore, it is likely that the electronic structure at around $(\pi,0)$ becomes coherent below T^* while the pseudogap opens in the different region of the k space. This is consistent with results of the low-T angle-resolved photoemission spectra,[24–26] which revealed pseudogap formation at around $(\pi/2,\pi/2)$ and the presence of a small electron pocket (or Fermi arc) at around $(\pi,0)$ at low T in the underdoped region. The B_{1g} Raman scattering spectra have also been investigated for the $Nd_{2-x}Ce_xCuO_4$ crystals $(0 \leqslant x \leqslant 0.15)$. The intensity of the two-magnon peak in the underdoped region ($x = 0.05,\ 0.10$) increases rapidly below T^*. This result also suggests that the origin of the pseudogap is due to the evolution of antiferromagnetic spin correlation.

ACKNOWLEDGMENTS

The authors thank N. Nagaosa, H. Takagi, T. Tohyama, Z.-X. Shen, and S. Maekawa for enlightening discussions. The present work was in part supported by a Grant-In-Aid for Scientific Research from the MEXT and by the NEDO.

*Present address: Institute for Materials Research, Tohoku University, Sendai 980-8577, Japan.

[1] T. Timusk and B. Statt, Rep. Prog. Phys. **62**, 61 (1999) and references cited therein.

[2] D.S. Marshall, D.S. Dessau, A.G. Loeser, C-H. Park, A.Y. Matsuura, J. N. Eckstein, I. Bozovic, P. Fournier, A. Kapitulnik, W.E. Spicer, and Z.-X. Shen, Phys. Rev. Lett. **76**, 4841 (1996).

[3] F. Ronning, C. Kim, D.L. Feng, D.S. Marshall, A.G. Loeser, L.L. Miller, J.N. Eckstein, I. Bozovic, and Z.X. Shen, Science **282**, 2067 (1998).

[4] A. Ino, T. Mizokawa, K. Kobayashi, A. Fujimori, T. Sasagawa, T. Kimura, K. Kishio, K. Tamasaku, H. Eisaki, and S. Uchida, Phys. Rev. Lett. **81**, 2124 (1998).

[5] T. Sato, T. Yokoya, Y. Naitoh, T. Takahashi, K. Yamada, and Y. Endoh, Phys. Rev. Lett. **83**, 2254 (1999).

[6] H. Ding, T. Yokoya, J.C. Campuzano, T. Takahashi, M. Randeria, M.R. Norman, T. Mochiku, K. Kadowaki, and J. Giapintzakis, Nature (London) **382**, 51 (1996).

[7] A.G. Loeser, Z.X. Shen, D.S. Dessau, D.S. Marshall, C.H. Park, P. Fournier, and A. Kapitulnik, Science **273**, 325 (1996).

[8] Ch. Renner, B. Revaz, J.-Y. Genoud, K. Kadowaki, and Ø. Fischer, Phys. Rev. Lett. **80**, 149 (1997).

[9] J.D. Takeda, T. Nishikawa, and M. Sato, Physica C **231**, 293 (1994).

[10] H.Y. Hwang, B. Batlogg, H. Takagi, H.L. Kao, J. Kwo, R.J. Cava, J.J. Krajewski, and W.F. Peck, Jr., Phys. Rev. Lett. **72**, 2636 (1994).

[11] H. Takagi, T. Ido, S. Ishibashi, M. Uota, S. Uchida, and Y. Tokura, Phys. Rev. B **40**, 2254 (1989).

[12] T. Nakano, M. Oda, C. Manabe, N. Momono, Y. Miura, and M. Ido, Phys. Rev. B **49**, 16 000 (1994).

[13] H. Yasuoka, T. Imai, and T. Shimizu, in *Strong Correlation and Superconductivity*, edited by H. Fukuyama, S. Maekawa, A.P. Malozemoff (Springer-Verlag, Berlin, 1989), p. 254.

[14] J. Rossat-Mignod, L.P. Regnault, C. Vettier, P. Bourges, P. Burlet, J. Bossy, J.Y. Henry, and G. Lapertot, Physica C **185-189**, 86 (1991).

[15] Y. Tokura, H. Takagi, and S. Uchida, Nature (London) **337**, 345 (1989).

[16] P.W. Anderson, Science **256**, 1526 (1992).

[17] E. Dagotto, Rev. Mod. Phys. **66**, 763 (1994).

[18] J.B. Torrance, Y. Tokura, A.I. Nazzal, A. Bezinge, T.C. Huang, and S.S.P. Parkin, Phys. Rev. Lett. **61**, 1127 (1988).

[19] G.M. Luke, L.P. Le, B.J. Sternlieb, Y.J. Uemura, J.H. Brewer, R. Kadono, R.F. Kiefl, S.R. Kreitzman, T.M. Riseman, C.E. Stronach, M.R. Davis, S. Uchida, H. Takagi, Y. Tokura, Y. Hidaka, T. Murakami, J. Gopalakrishnan, A.W. Sleight, M.A. Subramanian, E.A. Early, J.T. Markert, M.B. Maple, and C.L. Seaman, Phys. Rev. B **42**, 7981 (1990).

[20] Recently, a pseudogap as large as superconducting gap has been discerned under high magnetic field above H_c (Ref. 21). This pseudogap is much smaller than the present pseudogap and may correspond to the smaller pseudogap as in the hole-doped system.

[21] L. Alff, Y. Krockenberger, B. Welter, M. Schonecke, R. Gross, D. Manske, and M. Naito, Nature (London) **422**, 698 (2003).

[22] Y. Onose, Y. Taguchi, T. Ishikawa, S. Shinomori, K. Ishizaka, and Y. Tokura, Phys. Rev. Lett. **82**, 5120 (1999).

[23] Y. Onose, Y. Taguchi, K. Ishizaka, and Y. Tokura, Phys. Rev. Lett. **87**, 217001 (2001).

[24] N.P. Armitage, D.H. Lu, D.L. Feng, C. Kim, A. Damascelli, K.M. Shen, F. Ronning, Z.X. Shen, Y. Onose, Y. Taguchi, and Y. Tokura, Phys. Rev. Lett. **86**, 1126 (2001).

[25] N.P. Armitage, D.H. Lu, C. Kim, A. Damascelli, K.M. Shen, F. Ronning, D.L. Feng, P. Bogdanov, Z.X. Shen, Y. Onose, Y. Taguchi, Y. Tokura, P.K. Mang, N. Kaneko, and M. Greven, Phys. Rev. Lett. **87**, 147003 (2001).

[26] N.P. Armitage, F. Ronning, D.H. Lu, C. Kim, A. Damascelli, K.M. Shen, D.L. Feng, H. Eisaki, Z.-X. Shen, P.K. Mang, N. Kaneko, M. Greven, Y. Onose, Y. Taguchi, and Y. Tokura, Phys. Rev. Lett. **88**, 257001 (2002).

[27] A.J. Schultz, J.D. Jorgensen, J.L. Peng, and R.L. Greene, Phys. Rev. B **53**, 5157 (1996).

[28] E.J. Singley, D.N. Basov, K. Kurahashi, T. Uefuji, and K. Yamada, Phys. Rev. B **64**, 224503 (2001).

[29] C.C. Homes, B.P. Clayman, J.L. Peng, and R.L. Greene, Phys. Rev. B **56**, 5525 (1997).

[30] J.P. Falck, A. Levy, M.A. Kastner, and R.J. Birgeneau, Phys. Rev. Lett. **69**, 1109 (1992).

[31] H.S. Choi, Y.S. Lee, T.W. Noh, E.J. Choi, Y. Bang, and Y.J. Kim, Phys. Rev. B **60**, 4646 (1999).

[32] S.L. Cooper, G.A. Thomas, J. Orenstein, D.H. Rapkine, A.J. Millis, S.W. Cheong, A.S. Cooper, and Z. Fisk, Phys. Rev. B **41**, 11 605 (1990).

[33] T. Arima, Y. Tokura, and S. Uchida, Phys. Rev. B **48**, 6597 (1993).

[34] S. Uchida, T. Ido, H. Takagi, T. Arima, Y. Tokura, and S. Tajima, Phys. Rev. B **43**, 7942 (1991).

[35] M. Imada, A. Fujimori, and Y. Tokura, Rev. Mod. Phys. **70**, 1039 (1998).

[36] S. Sugai, T. Kobayashi, and J. Akimitsu, Phys. Rev. B **40**, 2686 (1989).

[37] M. Matsuda, K. Yamada, K. Kakurai, H. Kadowaki, T.R. Thurston, Y. Endoh, Y. Hidaka, R.J. Birgeneau, M.A. Kastner, P.M. Gehring, A.H. Moudden, and G. Shirane, Phys. Rev. B **42**, 10 098 (1990).

[38] A.V. Puchkov, D.N. Basov, and T. Timusk, J. Phys.: Condens. Matter **8**, 10049 (1996).

[39] Heyen *et al.* assigned the 0.037 eV mode to the Cu-O bending mode and the 0.042 eV mode to the Nd-O vibration mode (Ref. 40). However, the 0.037 eV mode hardly couples with the electronic continuum while the other modes show Fano-type antiresonance in the doped crystal. Hence, we assign here the 0.037 eV mode to the Nd-O vibration mode and the 0.042 eV mode to Cu-O bending mode, which is consistent with the assignment by Tajima *et al.* (Ref. 41). As for the 0.016 eV mode and the 0.063 eV mode, we follow the assignments of Heyen *et al.*

[40] E.T. Heyen, G. Kliche, W. Kress, W. Konig, M. Cardona, E. Rampf, J. Prade, U. Schroder, A.D. Kulkarni, F.W. de Wette, S. Pinol, D. McK Paul, E. Moran, and M.A. Alario-Franco, Solid State Commun. **74**, 1299 (1990).

[41] S. Tajima, T. Ido, S. Ishibashi, T. Itoh, H. Eisaki, Y. Mizuo, T. Arima, H. Takagi, and S. Uchida, Phys. Rev. B **43**, 10 496 (1991).

[42] U. Fano, Phys. Rev. **124**, 1866 (1961).

[43] See Fig. 3 and the related description of Ref. 38.

[44] A. Kaminski, J. Mesot, H. Fretwell, J.C. Campuzano, M.R. Norman, M. Randeria, H. Ding, T. Sato, T. Takahashi, T. Mochiku, K. Kadowaki, and H. Hoechst, Phys. Rev. Lett. **84**, 1788 (2000).

[45] A. Lanzara, P.V. Bogdanov, X.J. Zhou, S.A. Keller, D.L. Feng, E.D. Lu, T. Yoshida, H. Eisaki, A. Fujimori, K. Kishio, J.I. Shimoyama, T. Noda, S. Uchida, Z. Hussain, and Z.X. Shen, Nature (London) **412**, 510 (2001).

[46] T. Sato, T. Kamiyama, T. Takahashi, K. Kurahashi, and K. Yamada, Science **291**, 1517 (2001).

[47] N.P. Armitage, D.H. Lu, C. Kim, A. Damascelli, K.M. Shen, F. Ronning, D.L. Feng, P. Bogdanov, X.J. Zhou, W.L. Yang, Z. Hussain, P.K. Mang, N. Kaneko, M. Greven, Y. Onose, Y. Taguchi, Y. Tokura, and Z.X. Shen, Phys. Rev. B **68**, 064517 (2003).

[48] S. Uchida, K. Tamasaku, and S. Tajima, Phys. Rev. B **53**, 14 558 (1996).

[49] H. Takagi, Y. Tokura, and S. Uchida, Physica C **162-164**, 1001 (1989).

[50] C.C. Tsuei, A. Gupta, and G. Koren, Physica C **161**, 415 (1989).

[51] S.J. Hagen, X.Q. Xu, W. Jiang, J.L. Peng, Z.Y. Li, and R.L. Greene, Phys. Rev. B **45**, 515 (1992).

[52] P. Fournier, J. Higgins, H. Balci, E. Maiser, C.J. Lobb, and R.L. Greene, Phys. Rev. B **62**, R11 993 (2000).

[53] B. Bucher, P. Steiner, J. Karpinski, E. Kaldis, and P. Wachter, Phys. Rev. Lett. **70**, 2012 (1993).

[54] T. Ito, K. Takenaka, and S. Uchida, Phys. Rev. Lett. **70**, 3995 (1993).

[55] H. Takagi, S. Uchida, and Y. Tokura, Phys. Rev. Lett. **62**, 1197 (1989).

[56] ARPES spectra may be more sensitive to a gaplike structure compared with the optical spectra. This is typically seen in the underdoped region of hole-doped cuprates. A large pseudogap as large as hundreds meV is observed in the ARPES spectra of this region (Refs. 2–5) while such a large pseudogap has never been observed in the optical spectra (Ref. 38).

[57] K. Takenaka, K. Mizuhashi, H. Takagi, and S. Uchida, Phys. Rev. B **50**, 6534 (1994).

[58] O.K. Andersen, A.I. Liechtenstein, O. Jepsen, and F. Paulsen, J. Phys. Chem. Solids **56**, 1573 (1995).

[59] K. Yamada, K. Kuruhashi, Y. Endoh, R.J. Birgeneau, and G. Shirane, J. Phys. Chem. Solids **60**, 1025 (1999).

[60] M. Fujita, T. Kubo, S. Kuroshima, T. Uefuji, K. Kawashima, K. Yamada, I. Watanabe, and K. Nagamine, Phys. Rev. B **67**, 014514 (2003).

[61] H.J. Kang, P. Dai, J.W. Lynn, M. Matsuura, J.R. Thompson, S.C. Zhang, D.N. Argyriou, Y. Onose, and Y. Tokura, Nature (London) **423**, 522 (2003).

[62] For example, E. Fawcett, Rev. Mod. Phys. **60**, 209 (1988).

[63] T.R. Thurston, M. Matsuda, K. Kakurai, K. Yamada, Y. Endoh, R.J. Birgeneau, P.M. Gehring, Y. Hidaka, M.A. Kastner, T. Murakami, and G. Shirane, Phys. Rev. Lett. **65**, 263 (1990).

[64] The quantitative estimate of l is not appropriate for $x<0.10$ because Boltzman's theory cannot be applied to the case of $l<a$.

[65] I. Tomeno, M. Yoshida, K. Ikeda, K. Tai, K. Takamuku, N. Koshizuka, S. Tanaka, K. Oka, and H. Unoki, Phys. Rev. B **43**, 3009 (1991).

[66] T. Tohyama and S. Maekawa, Phys. Rev. B **64**, 212505 (2001).

[67] J. Schmalian, D. Pines, and B. Stojkovic, Phys. Rev. Lett. **80**, 3839 (1998).

[68] R.B. Laughlin, Phys. Rev. Lett. **79**, 1726 (1997).

[69] V.J. Emery, S.A. Kivelson, and O. Zachar, Phys. Rev. B **56**, 6120 (1997).